

## Focusing of shock waves

R. HOLL and H. GRÖNIG (AACHEN)

Experimental and theoretical studies of focused nonstationary spatial shock waves in air are presented. Weak spherical shock wave surfaces are generated by means of a spark discharge. They are converted to converging shock fronts by reflection at a concave wall. Schlieren and pressure measurements are used to study the spatial and time-dependent behaviour of these phenomena. The first results of simulation program and some modifications of available numerical methods are the subject of the final discussion.

Przeprowadzono eksperymentalne i teoretyczne badania problemu ogniskowania trójwymiarowych fal uderzeniowych w powietrzu. Powierzchnie słabych sferycznych fal uderzeniowych generowane są metodą iskrową. Ich transformacja na zbieżne fronty fal uderzeniowych następuje drogą odbicia od wklęsłej ścianki. Zastosowano obrazy schlierenowskie i pomiary ciśnienia dla wyjaśnienia przebiegu tego procesu w czasie i przestrzeni. Na zakończenie przedyskutowano pierwsze wyniki programu symulacyjnego i pewnych modyfikacji znanych metod numerycznych.

Проведены экспериментальные и теоретические исследования проблемы фокусирования трехмерных ударных волн в воздухе. Поверхности слабых сферических ударных волн генерируются искровым методом. Их преобразование в сходящиеся фронты ударных волн наступает путем отражения от вогнутой стенки. Применены шлирен-изображения и измерения давления для выяснения хода этого процесса во времени и в пространстве. В заключение обсуждены первые результаты имитационной программы и некоторых модификаций известных численных методов.

### 1. Introduction

THE FOCUSING of shock waves in air is of practical interest in various ways. For instance, destructions generated by turning or accelerating supersonic aircrafts may occur as well as failures of pressure vessels in chemical plants and reactors. The concentration of energy in converging shock waves may be responsible for those events.

First, a shock tube seems to be a suitable device in relevant experimental studies. The use of properly shaped end-wall reflectors makes possible the formation of converging waves. Corresponding experiments were performed by STURTEVANT and KULKARNY [1]. However, the pressure course across a shock wave in a shock tube is in general different from the pressure courses measured across a curved wave front in the free atmosphere. In the first case the pressure course is approximately a step function. In the latter case a sharp short-time rise of pressure and flow velocity is found, followed by a quick decay. In contrary to the shock tube, there hardly appears any mass flow into the area struck by the wave.

This behaviour equals the course of the flow properties in a blast wave of finite energy

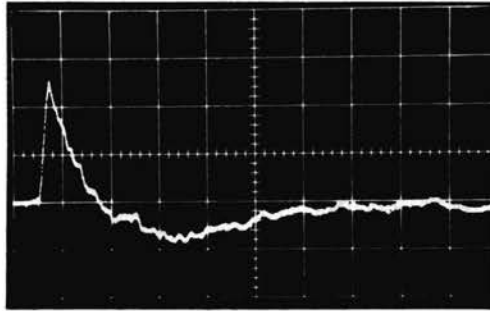


FIG. 1. Pressure history of a blast wave, horiz.:  $40 \mu\text{s}/\text{div}$ , vert.:  $0.1 \text{ b}/\text{div}$ .

at a larger distance from its origin. Figure 1 shows the characteristic pressure history of this waveform. Pressure rise and maximum amplitude are slightly falsified as a result of the finite dimensions of the pressure gauge.

## 2. Experimental setup

For the generation of weak blast waves an electric shock generator was constructed. A high voltage capacitor ( $35 \text{ kV}$ ;  $0.31 \mu\text{F}$ ) is discharged over a spark gap. The discharge consists of several damped oscillations. The radiated shock wave energy is proportional to the square of the current peak during the first quarter period of the discharge. Therefore a quick current rise should be reached. The periodic solution of the electric circuit delivers for the current rise

$$\left(\frac{dI}{dt}\right)_{t=0} = \frac{U_0}{L},$$

$U_0$  — discharge voltage,  $L$  — inductivity.

For the suppression of the following disturbing waves, the damping must be great enough. We have

$$\delta = \frac{R}{2L},$$

$R$  — resistance.

Both postulations can be realized by a low inductive design of the discharge circuit. Figure 2 shows the experimental setup. The conductors with replaceable electrodes are embedded in epoxy resin. The overall inductivity of the electric installation comes to  $71 \text{ nH}$ . A spherical shock front is generated (incident shock), which meets with a reflector at a distance of  $70 \text{ cm}$ . This is made out of a compound of epoxy resin and quartz powder. Its surface is part of an ellipsoid whose first focus coincides with the origin of the wave. Thus the shock front converges towards the second focus after reflection.

The shock fronts were photographed by means of a spark Schlieren apparatus with a  $180 \text{ mm}$  mirror diameter. Pressure histories were recorded by piezo pressure gauges. Figure 3 shows the expanding shock front  $120 \mu\text{s}$  after the discharge. At this time the pressure jump in the wave amounts to  $0.35b$ . The pressure discharge development conforms to Fig. 1.

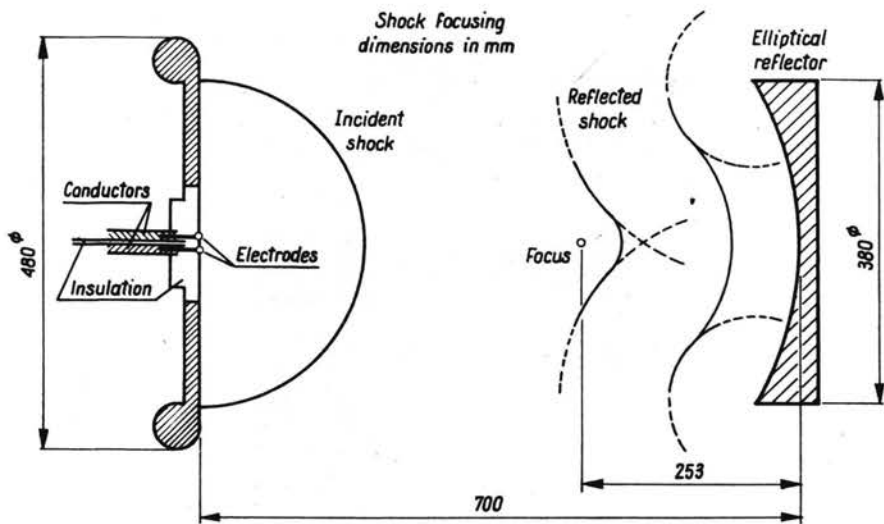


FIG. 2. Principle of the electric shock generation and focusing (dimensions in mm).



FIG. 3. Spherical shock front 120  $\mu$ s after discharge.



FIG. 4. Incident shock front (moving to the right).

### 3. Experimental results

Figure 4 shows the wave before the reflection. Figure 5 a short time after it. Both waves are spherical. The reflected wave has a decreased radius of curvature because it runs towards the second focus of the ellipsoid.

The reflection process at the reflector edge is visible in Fig. 6. The pressure history

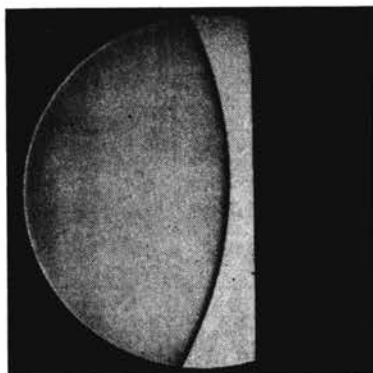
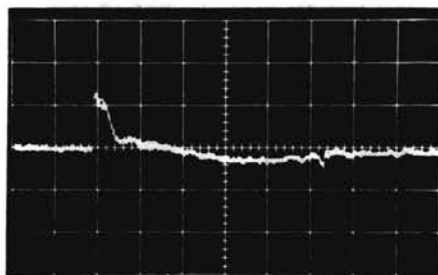


FIG. 5. Reflected shock front (moving to the left).



FIG. 6. Reflection at the reflector edge.



hor.:  $40 \mu\text{s}/\text{div}$       vert.:  $.025 \text{ b}/\text{div}$

FIG. 7. Pressure history at the centre of symmetry of the reflected wave. (True overpressure half as indicated).

on the axis of symmetry after reflection is shown in Fig. 7. As the pressure gauge was affected frontally, the real pressure variations are only half as great as indicated. This results in a maximum overpressure of  $\Delta p = 0.015b$  and an initial shock Mach number of 1.0064. Figures 8a–e show the focusing process. The field of view has a diameter of 178 mm. In Fig. 8b the geometrical focus of the ellipsoid is reached. Owing to the pressure amplification in the central focal region and subsequent acceleration, a levelling of this section occurs and a Mach-stem is formed (Fig. 8c). This nonlinear behaviour prevents

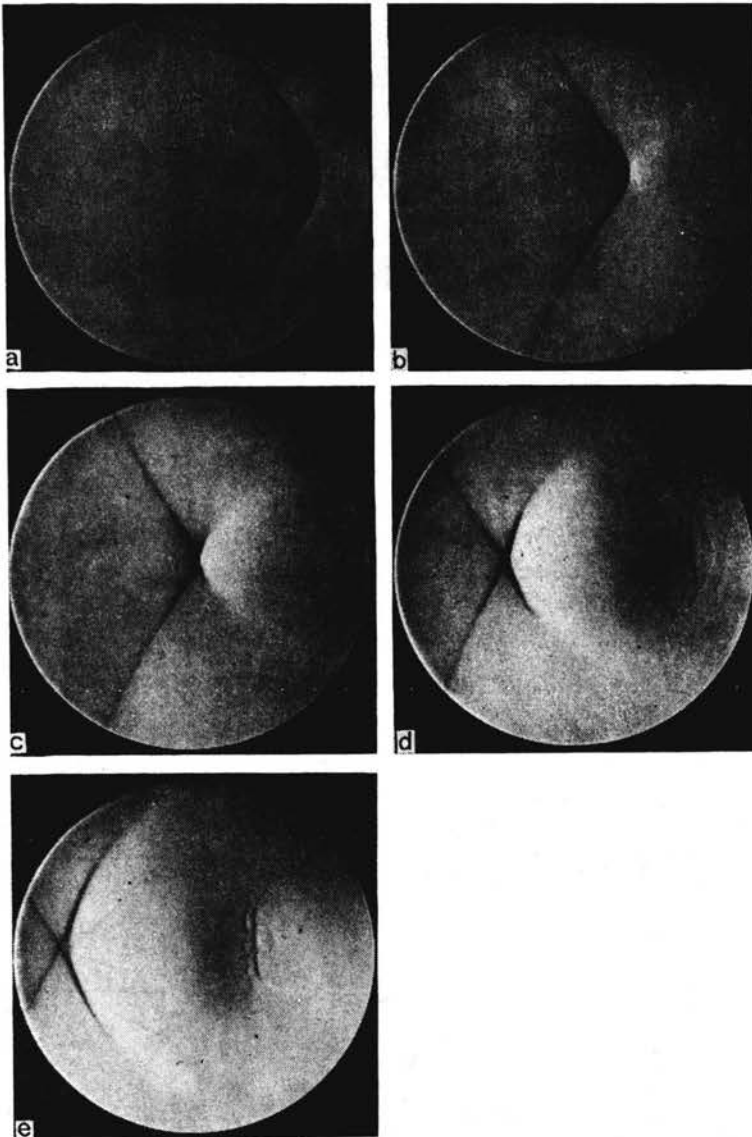
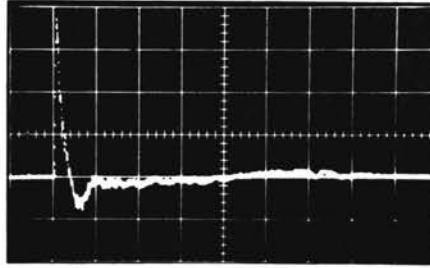


FIG. 8. Focusing process of an axisymmetric wave-front. Initial strength:  $M_0 = 1.0064$ , a) converging front, b) at the geometrical focus, c) Mach-stem, d) wave crossing, e) wave crossing with loop.

the formation of a point focus and limits the pressure amplification. Along with greater wave strength an increase of the Mach-stem is observed [1] after passing through the focus. In that case the shock front leaves the focal region with a slight convex profile. For weaker shocks the wave fronts cross one another on the Mach-stem as can be seen in Fig. 8d. They leave the focal region crossed and folded as predicted by geometrical acoustics (Fig. 8e). Figure 9 shows the pressure history at the geometrical focus. Again the pressure gauge was affected frontally. The true maximum overpressure is  $\Delta p = 0.334b$ . This yields an amplification factor of 22.



hor.: 40  $\mu$ s/div      vert.: .2 b/div

FIG. 9. Pressure history at the geometrical focus.

#### 4. Theory

Based on publications of WHITHAM [2], CHISNELL [3], and CHESTER [4], Davies and Guy developed an explicit numerical time stepping scheme which is shown in Fig. 10 for the case of a two-dimensional shock wave diffraction.

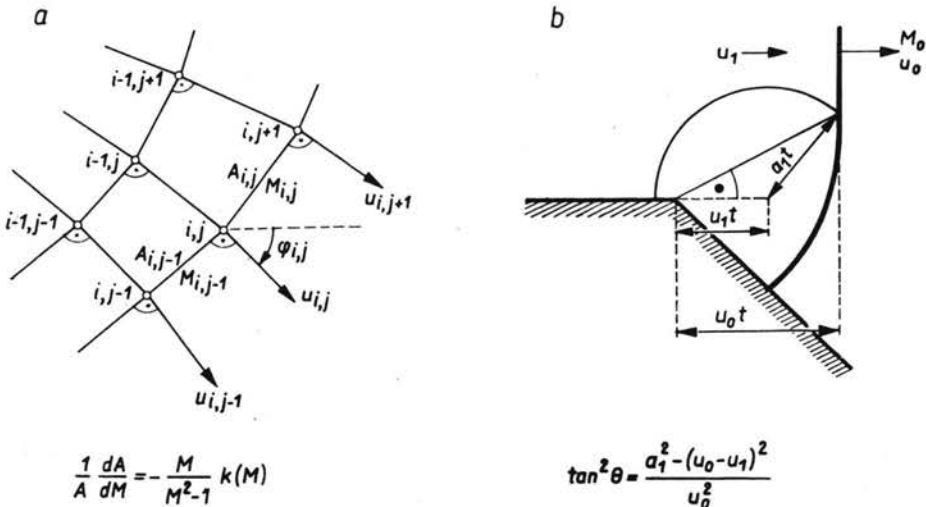


FIG. 10. Time stepping scheme (Davies/Guy) for shock diffraction.

Successive shock positions form with the local orthogonals, so-called rays, a mesh. Neighbouring rays are taken as channel walls between which the corresponding front element moves. The particular front elements are assumed to be straight and the familiar normal shock wave relations are applied to them. From the positions of the new mesh points the area changes are derived. Chisnell's formula (a) combines the area changes with the corresponding changes in Mach number. Thus the new strength distribution can be evaluated. Angle  $\theta$  determines the locus of the onset of diffraction on the incident shock front. It is defined by the point of intersection of the front and the sonic circle produced by the corner. The latter propagates with the local sound speed  $a_1$  in the wake of the incident shock. With slight modifications the described method was on trial, applied to the problem of shock focusing. Shock fronts and rays of a shock focusing process computed with the Davies/Guy method.

The results of two-dimensional calculations are shown in Figs. 11 and 12. The initial Mach numbers are 1.1 and 1.5, respectively. Each fiftieth wave front and each fifth mesh-point on a front are plotted. The geometrical focus is marked at the  $x$ -axis. The dimensions correspond to the data given in Fig. 2. The nonlinear levelling effect, the rise of a Machstem and the "overshooting" of the front region near the axis beyond the focus for  $M_0 = 1.5$  agree with experimental observations [1]. However, the results are only of qualitative significance. The respective reason and the indicated modifications of the computing method are discussed below.

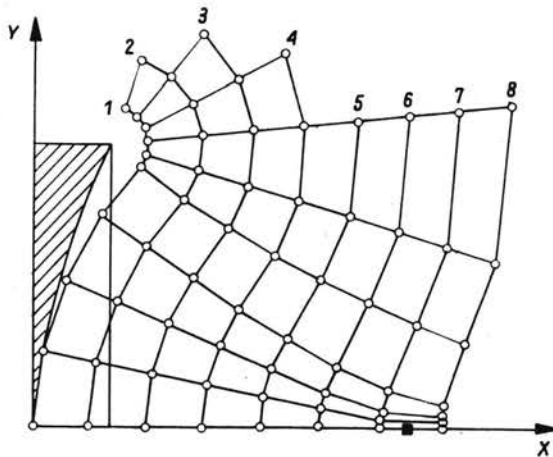


FIG. 11.  $M_0 = 1.1$ .

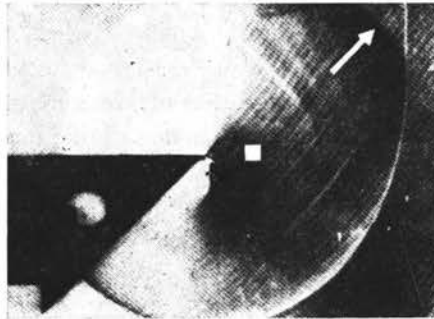
As indicated in Fig. 13 each point  $P$  of the shock front can be adjoined to a sphere of influence which determines the propagation velocity of disturbances along the front originating at  $P$ . If the shock front moves on by a distance  $U_0 \Delta t$ , the disturbances originated at  $P_{(t)}$  arrive in  $P_1$  and  $P_{-1}$ . The respective influence domain is hatched. Analytical and physical influence and dependence domains must agree or be restricted to the limitations of the latter. By the method of Davies and Guy, information can progress only by one front- and ray-distance each time step.



$$\int_0^{\Delta t} u_1(t) dt.$$

Its value has to be determined from the pressure course.

In order to examine these circumstances the diffraction of a blast wave by a convex corner was investigated with the shock generator and compared with corresponding shock tube experiments carried out by SKEWS [6]. Figure 14 shows a Schlieren picture taken by Skews for a shock Mach number  $M_0 = 1.2$ . The arrow points at the sonic circle whose centre (square) is distinctly carried off to the right by the wake. Figure 15 shows a blast



$M_0 = 1.20$

FIG. 14. Diffraction of a shock wave measured in a shock tube:  $M_0 = 1.2$  (Skews).

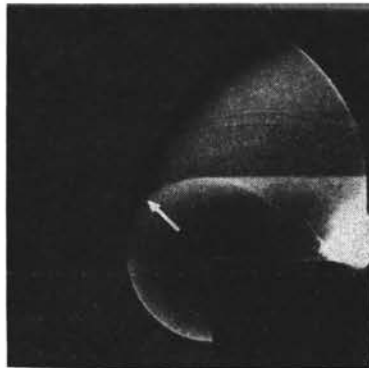


FIG. 15. Diffraction of a blast wave in free atmosphere;  $M_0 = 1.14$ .

wave produced by the shock generator and diffracted at a cylinder edge. Again the sonic circle is marked by an arrow. The Mach number of the incident shock is 1.14, the pressure course corresponds to that of Fig. 1. For the Mach number of 1.14 a shock tube experiment yields a ratio  $u_1 t / u_0 t = 0.19$  (Fig. 10(b)) while in Fig. 15 the ratio of the corresponding distances is about 0.06, that is the centre of the sonic circle remains nearly at the edge.

#### 4. Conclusions

The finally presented reflections and experiments reveal that the shock pressure course influences the temporal development of a curved shock front. This is not taken into account by the method of Davies and Guy. Moreover, since its application to focusing processes led to ray crossing which could be eliminated only by violating the influence domains, the following modifications of the method shall be examined:

After each time step there follows a new covering of the front with mesh points. Hereby the ratios of the point- and front intervals and with this the influence domains can be adapted to the shock pressure profile and the local Mach number. The latter is derived from an interpolation over the old neighbouring points. This procedure additionally causes a numerical smoothening whereby program instabilities, which might lead to ray crossing, do not increase. Of course this smoothening must operate only locally in dimensions that are small as compared with the local radius of curvature of the shock front. An estimate of the margins of error for linear interpolation during the new covering with points yielded that for a sufficient fine mesh the accumulated error remains negligibly small.

#### References

1. B. STURTEVANT, V. A. KULKARNY, *The focusing of weak shock waves*, J. Fluid Mech., 73, part, 4, 651-671, 1976.
2. G. B. WHITHAM, *A new approach to problems of shock dynamics, Part I. Two-dimensional problems*, J. Fluid Mech., 2, 145-171, 1957.
3. R. F. CHISNELL, *The motion of a shock wave in a channel with applications to cylindrical and spherical shock waves*, J. Fluid Mech., 2, 286-298, 1957.
4. W. CHESTER, *The propagation of shock waves in a channel of non-uniform width*, Quart. J. Appl. Math. 6, 440-452, 1953.
5. P. O. A. L. DAVIES, T. B. GUY, *The prediction of weak diffracting and reflecting wave patterns*, Z. Flugwiss., 19, 8/9, 339-347, 1971.
6. B. W. SKEWS, *The perturbed region behind a diffracting shock wave*, J. Fluid Mech., 29, 4, 705-719, 1967.

TECHNISCHE UNIVERSITÄT, AACHEN, BRD.

Received October 22, 1981.